



Antimicrobial and Photo Degradation activity of Synthesized BiVO_4 Nanocrystals

M.Sangareswari^{1&3*}, S. Arul Manikandan², T. Adinaveen⁴, S. Srinivasan⁴, S. Sathyakumar⁴, M. Srinivasan⁴, P. Ganapathy⁴ and Jiji George⁵

1)PG and Research Department of Chemistry, Dhanalakshmi Srinivasan College of Arts and Science for Women (Autonomous), Perambalur- 621 212, Tamilnadu, India

2)Dhanalakshmi Srinivasan University, Trichy-621112, Tamilnadu, India

3)Centre for Research and Post Graduate Studies in Chemistry, Ayya Nadar Janaki Ammal College, Sivakasi - 626 124, Tamilnadu, India

⁵Prof. & Head, Babu Banarasi Das University, Lucknow, U.P., INDIA

Email: srisangari5@gmail.com

ABSTRACT

The present study investigates the photo catalytic degradation of Methylene blue (MB) and Rhodamine B (Rh B) dyes under sunlight irradiation. The BiVO_4 material was synthesized by sonochemical method. The surface morphology of the prepared material was analysed by Scanning Electron Microscopy and Transmission Electron microscopy. The crystal structure of the prepared material was analysed by X-ray diffraction analysis. The band gap of the prepared material was calculated by $2.2e\text{ V}$ by using Tauc's plot. The functional group of the prepared the material was analysed by Fourier Transform Infra red spectroscopy. The advantage of the prepared BiVO_4 nanocrystals is having a higher photo catalytic activity due to its lower band gap. An attempt has been made to study the various parameters like concentration, pH, dose and time variation for the two dyes under sunlight irradiation. The percentage removal of dyes can be measured by using UV-Visible spectrophotometer. The possible photocatalytic mechanism also investigated. The visible light driven BiVO_4 nanoparticles interact with sunlight to produce a number of holes and electrons on the surface of VB and CB on BiVO_4 photocatalyst. The superoxide and hydroxyl radicals are responsible for degradation of dyes. The O_2 and OH radicals will degrade the dye into minerals like water and CO_2 . The stability of the material was also investigated by using number of cycling.

Keywords: BiVO_4 nanocrystals; Methylene Blue; Rhodamine B; Zero point charge; sunlight, dose, UV-Visible

Received 22.10.2022

Revised 12.11.2022

Accepted 16.12.2022

INTRODUCTION

With the rapid development of industrialization, urbanization as well as population, the urgent demand and acute shortage of clean water sources have attracted great attention all over the world [1]. Water purification is of great significance in alleviating the increasingly serious water resource crisis as well as tackling the growing concern over the water contamination [2]. Dyes from the industrial waste one of the major problems for environmental pollution [3]. Now - a - days photo catalysis is expected to play an important role in both environmental pollution as well as water splitting for hydrogen production [4-5]. TiO_2 and ZnO both are efficient photo catalyst for dye degradation. But they have some limitations of their photo catalytic activity. They only active under UV excitation because of its large band gap energy $\sim 3.2\text{ eV}$ [6]. The success of photo catalytic reactions greatly depends on the proper selection of catalyst materials. In this regard, bismuth vanadate (BiVO_4) has attracted considerable interest to date due to its narrow band gap, non-toxicity, high stability, and advanced sunlight- harvesting capacity [7]. Recently the development of visible-light driven photo catalyst has attracted more attention. Among these, one of the promising non-Titania based visible-light driven semiconductor photocatalyst is BiVO_4 [8-10]. Methylene Blue (MB) is an ionic heterocyclic organic compound with high biochemical stability, relatively high molecular weight, and high water solubility, and it cause permanent injury to humans and animals on inhalation and ingestion. Rhodamine B is a dye that belongs to a class of compounds called Xanthenes, extensively region of the electromagnetic spectrum. This dye is currently used as dye laser material and is part of the triphenylmethane family of dyes that contain four N-ethyl groups at both sides of the xanthene rings. The structure of both Rh B and MB was depicted as Fig. 1 (a,b). Thus, in this study, the photo catalytic treatment of MB and Rh B in aqueous solutions was chosen as model pollutants to evaluate the activity of target composite photo catalysts.

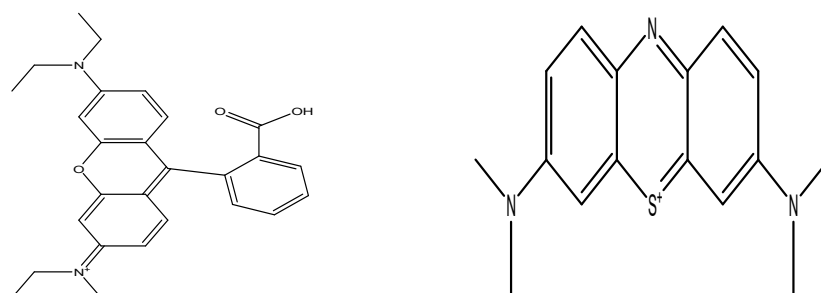


Fig. 1 Structure of Rhodamine B (a) and Methylene Blue (b)

MATERIAL AND METHODS

Chemicals

The Chemical Bismuth Nitrate pentahydrate purchased from Merck, Ammonium meta vanadate and Ammonium persulfate purchased from Thomas Baker Chemicals, Methylene Blue and Rhodamine B dyes from Qualigens Fine Chemicals. The Pyrrole (98+%) obtained from Alfa Aesar, Ethylene glycol reagent from S. D. Fine Chemicals. All the other chemicals and reagents were analytical grade used without further purification.

Synthesis of sunlight driven BiVO₄ nanocrystals

0.1M Bi (NO₃). 5H₂O and 0.1 M NH₄VO₃ were mixed together in 100ml solvent containing ethylene glycol and deionised water. Then the mixture was then stirred for 1h at room temperature to get a solution. Afterwards, the mixture was exposed to high-intensity ultrasonic irradiation (600W, 20kHz) at room temperature in ambient air for 2h. The yellow precipitate was centrifuged, washed with DD water and absolute ethanol and then dried at 343K for 10h in the air.

Equipment

UV-visible spectrophotometer (DRS) was recorded using "SHIMADZU" model: UV 2450, FT-IR spectrum was recorded using "SHIMADZU" (Model: 8400S). The Crystallographic structures of the materials were determined by High resolution powder diffractometer model - RICH SIEFRT & CO with Cu as the X-ray source ($\lambda=1.5406 \times 10^{-10}$ m). The surface morphology of the sample was recorded using Scanning Electron Microscopy and Energy Dispersive X-ray Analysis (SEM-EDAX) (Model: FEG Quantum 250 EDAX) and Transmission Electron Microscopy.

Photocatalytic activity

Photo catalytic activities of the prepared BiVO₄ nanocrystals were evaluated by the degradation of MB and Rh B dyes under sunlight irradiation. In each experiment, the 0.4g/L amount of photo catalyst was added into Rhodamine B ($\lambda_{\max} = 552$ nm) and Methylene Blue ($\lambda_{\max} = 665$ nm) solution. Prior to irradiation, the suspensions were stirred in the dark for 1 h to reach an adsorption/desorption equilibrium between the pollutant and photo catalyst. Under irradiation, the suspensions were stirred continuously and open to air. At irradiation time intervals of 1 h, 4mL of the suspensions were collected, and then centrifuged to remove the photo catalyst particles. The solutions were analyzed by a UV-vis spectrophotometer and the absorbance at 552 nm and 665nm were monitored.

The photo catalytic efficiency of the synthesized BiVO₄ nanocrystals was calculated by using the formula, Percentage removal (% R) = $100 \times (C_0 - C_t) / C_0$

Where,

C₀ = initial concentration of dye (ppm)

C_t = final concentration of dye (ppm) at given time

RESULT AND DISCUSSION

Surface morphology of BiVO₄ nanocrystals

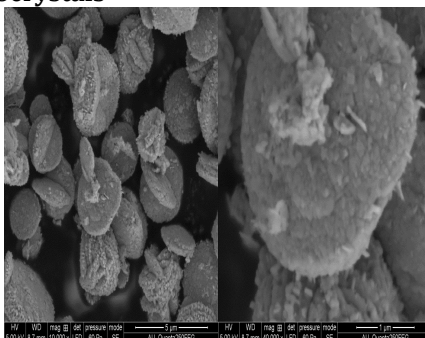


Fig.2 SEM image of BiVO₄ Photocatalyst

The Surface morphology of the synthesised BiVO_4 Photo catalyst is shown in Fig. 2. The seed like structure of the crystal material is clearly observed in the SEM image with crystalline like surfaces. However, the surfaces of the particles are very loose. This kind of surface structure can provide a better adsorption environment and a more active site for the photo catalytic reaction. The agglomeration occurs at the interfaces is due to electrostatic forces and Vanderwaal's interactions. [12-14].

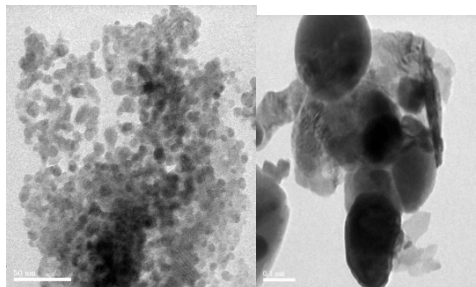


Fig.3 TEM analysis of BiVO_4 Photocatalyst

The TEM images for the synthesised BiVO_4 photo catalyst are shown in Fig. 3. The particles are having spherical shape. They are well matched with the SEM analysis.

EDAX analysis

The composition of the BiVO_4 material was confirmed by analyzing EDAX spectrum. The exhibited peaks correspond to C, O, V and Bi which are present in the BiVO_4 Photo catalyst. The impurities like Fe and Br are also present in EDAX spectrum. Among these elements Bismuth ions present in higher weight percentages (44.32%) as shown in Fig.4.

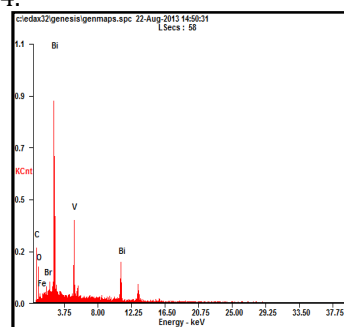


Fig.4 EDAX analysis of BiVO_4 Photocatalyst

Crystal structure of BiVO_4 nanocrystals

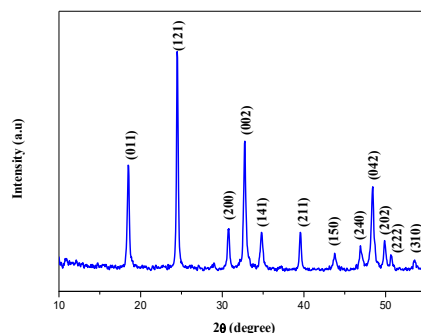


Fig.5 XRD pattern for BiVO_4 Photocatalyst

Fig. 5 shows the XRD diagram of BiVO_4 nanocrystals. The XRD peaks of BiVO_4 nanocrystals at 2θ of 18.68° , 25.8° , 28.85° , 30.54° , 35.45° , 39.9° , 42.40° , 47.0° , 47.5° , 50.00° , 50.26° and 53.7° were indexed as (011), (121), (200), (002), (141), (211), (150), (240), (042), (202), (222) and (310) planes according to JCPDS [12-19]. By increasing the calcinations temperature the (121) peak of BiVO_4 has become sharper, which indicates the dependence of crystalline to the applied temperature. The sharp and narrow diffraction peaks indicated a high crystallinity of the BiVO_4 . No other impurities such as Bi_2O_3 , V_2O_5 , or other organic compounds related to reactants were detected, indicating the high phase purity of the BiVO_4 samples. The average crystallite size of BiVO_4 nanoparticles was about 6.66 nm calculated according to Scherrer's equation.

Band gap of BiVO₄ nanocrystals

The optical absorption properties of BiVO₄ nanocrystals were determined by using UV-Diffuse reflectance spectrum as shown in Fig. 6. From that spectrum the band gap for the prepared BiVO₄ nanocrystals was calculated. The position of the fundamental absorption edge of BiVO₄ nanocrystals was determined using equation, $E_g = hc/\lambda$. The band gap of the as prepared BiVO₄ nanocrystal is 2.2eV, which represents that due to its lower band gap the catalyst will act as a semiconductor. So it will easily conduct the electrons from Valance band to Conduction band. The BiVO₄ nanocrystals can be excited to produce more electron - hole pairs under visible light illumination, which could result in higher photocatalytic activities. [20-23].

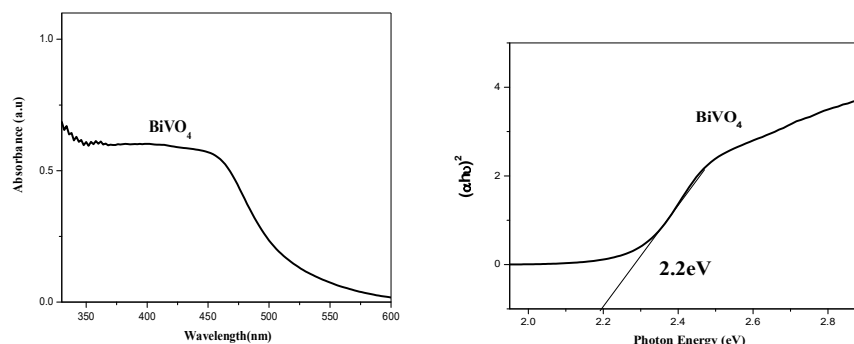


Fig. 6a UV-DRS for BiVO₄ Photocatalyst Fig.6b Tauc plot for BiVO₄ Photocatalyst

FT-IR spectrum for BiVO₄ nanocrystals

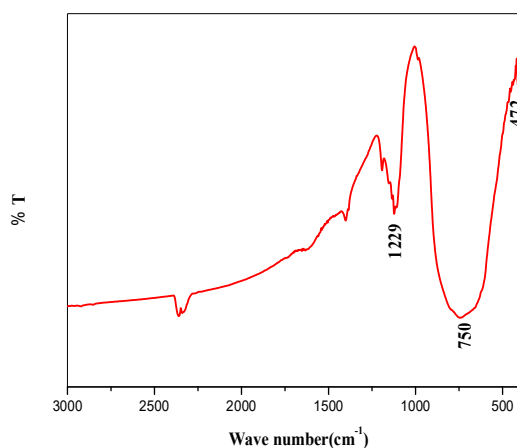


Fig.7 FTIR Spectrum of BiVO₄ Photocatalyst

The FT-IR spectrum of the synthesized BiVO₄ nanocrystals as shown in Fig.7. The peak occurs at 472 cm⁻¹ which denote the symmetric stretching vibration for VO₄³⁻. The broadband occurs from 650 to 850 cm⁻¹ multiple characteristic bands which denote the stretching and bending vibration band of Bi-O and V-O respectively [24-30].

Zero point charge

The aqueous suspension of adsorbent material (100mg in 50ml) is prepared in 50 ml solution of NaNO₃ of concentration 0.001N. Aliquots of suspension are adjusted to various pH values by the addition of dilute solution of sodium hydroxide of Nitric acid of strength 1.0 N. After 60 min, equilibrium at 30 ± 1° C in a thermostatic mechanical orbit shaker. The pH value (initial pH) is measured with a pen type digital pH meter. Then, one gram of sodium nitrate is added to an aliquot in each bottle, to bring a final electrolyte concentration to about 0.45 M. After an additional 60 min agitation, the final pH is measured by pen type digital pH meter. The ΔpH (ΔpH = Final pH - Initial pH) is calculated and plotted against solution pH. Typical plots of ΔpH Vs pH of the solution are obtained for the determination of zero point charge (pH_{ZPC}). The pH at which the ΔpH = 0, yielded pH_{ZPC} value at zero point charge. The zero point charge for the synthesized BiVO₄ nanocrystals 3.0. as illustrated as Table.1 [31-35]

Table 1 Table 1 Zero point charge for BiVO₄ Photocatalyst

pH before shaking (pH)	pH after shaking (Δ pH)	Zero point charge ZPC= (Δ pH - pH)
2	2.9	0.9
3	3.0	0
4	5.0	1
5	5.9	0.9
6	8.3	2.3
7	6.8	0.2
8	8.2	0.2
9	7.0	2.0
10	8.8	1.2
11	9.8	1.3

Photodegradation of dyes using BiVO₄ nanocrystals**Effect of initial concentration of dye****Table 2** Photodegradation of MB and RhB dyes under sunlight irradiation at different concentration

Concentration (ppm)	% Removal of MB dye	% Removal of Rh B dye
2	58.71	50.25
4	47.32	45.14
6	40.34	38.16
8	35.40	30.19
10	29.52	25.06
12	25.04	20.19

The Concentration of the two dyes increased from 1 to 6ppm as shown in Table.2 When the concentration of dye increases the percentage removal of dye was decreased, because the number of dye molecules which are adsorbed on the surface of Photo catalyst. The hydroxyl radical is the strongest oxidizing agent promoting the degradation rate. According to beer-Lambert law, as the initial dye concentration increases, the path length of the photon entering the solution decreases therefore resulting lower photo degradation rate. [36-38]

Effect of time varies**Table 3** Photodegradation of MB and RhB dyes under sunlight irradiation at different time

Time (min)	% Removal of MB dye	% Removal of Rh B dye
15	5.32	4.5
30	12.75	10.71
45	30.56	15.27
60	40.45	35.28
75	47.12	42.17
90	57.23	50.04

The effect of contact time on the amount of MB and Rh B dye adsorbed was investigated using the fixed initial concentration with 0.4g/l of BiVO₄ nanocrystals, respectively. It was observed that the adsorption percentage was found to be increased with increasing the time as shown in Table.3. The degradation of MB is faster than that of Rh B dye which can be explained by the fact that the MB molecules were close to a stripe shape, so they were easier to be absorbed in the same direction as the pure path of the catalyst. But in Rh B dye side tropism adsorption was occurring. So the percentage removal of Rh B dye was lower than compared to MB dye. It was considered that the sorption of the dye is an important parameter in determining the photo catalytic degradation rate. The kinetic plot for MB and Rh B dye as illustrated as Fig.8 [39-43].

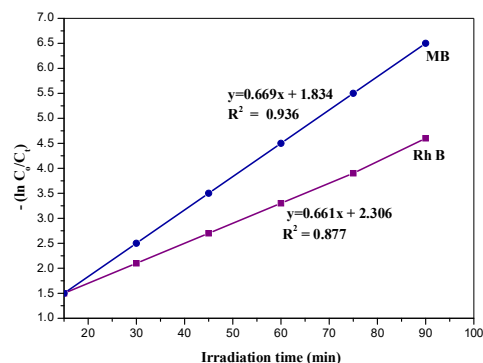


Fig. 8 Kinetics plot for MB and RhB degradation

Effect of dose variation

Table 4 Photodegradation of MB and RhB dyes under sunlight irradiation at different dosage

Dose (mg)	% Removal of MB dye	% Removal of Rh B dye
10	10.25	7.26
12	12.75	10.71
14	25.34	20.78
16	35.75	27.34
18	40.25	34.70
20	57.80	51.02

The photo catalyst of BiVO_4 nanocrystals, which are responsible for photo gradation of MB and Rh B dyes. The catalyst amount increases from 10mg to 20mg the percentage removal of dye will be increased as illustrated as Table.4. However, when photo catalyst was overdosed, the number of active sites on the photo catalysts surface may become almost constant because of the decreased light penetration, the increased light scattering and the loss in surface area occasioned by agglomeration at high solid concentration.

Effect of pH variation

Table 5 Photodegradation of MB and RhB dyes under sunlight irradiation at different pH

pH	% Removal of MB dye	% Removal of Rh B dye
1	80	70
3	73	60
5	54	50
7	42	40
9	31	25
11	15	5

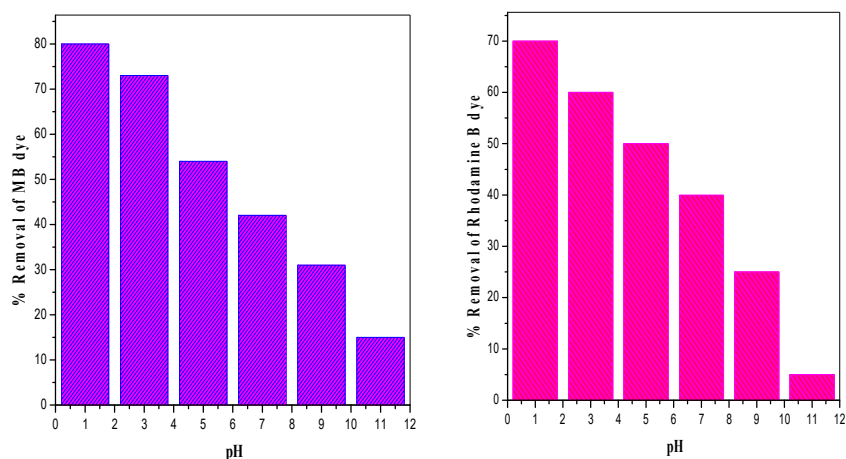


Fig.9 pH variation for a) MB dye b) RhB dye

The effect of pH variation is one of the important factors for photo degradation of dyes. The pH increases from 3 to 11 for both MB and Rh B dyes. The zero point charge for BiVO₄ nanocrystals was 3.0. At lower pH value is) pH 3 the % removal of dye degradation increases which showed in Table. 5. When the pH value increases from 5 to 11 the % removal of dye will be decreased. The pH of the solution is below 3.0 the surface of the active catalyst will become positively charged so the dye removal percentage increases. At higher pH value the surface of the catalyst will be negatively charged. So the % removal of dye will be decreased is illustrated in Fig.9

Mechanism

The visible light driven BiVO₄ nanoparticles interact with sunlight to produce a number of holes and electrons on the surface of VB and CB on BiVO₄ photocatalyst. The superoxide and hydroxyl radicals are responsible for degradation of dyes. The O₂^{•-} and OH[•] radicals will degrade the dye into minerals like water and CO₂. The described mechanism as illustrated in Fig. 10.

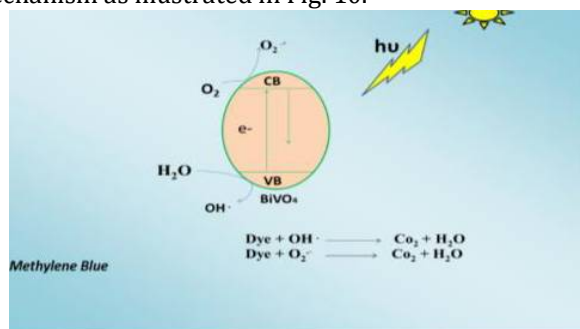


Fig.10 Mechanism for Photodegradation of Dye

Stability of catalyst

The reproducibility of the photo catalyst was also studied. After the first catalytic test, the catalyst was removed from aqueous solution, and then it was washed with ethanol and distilled water and dried at room temperature. After each use, no significant decrease of photo catalytic activity was observed after reuse for 4 times, which suggested that the active sites on the surface of this composite might be occupied by the products and reactants during filtration. No significant loss of activity was found in four successive runs as shown in Fig.11.

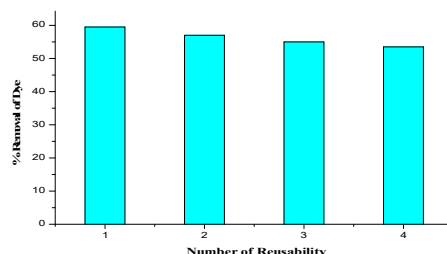


Fig. 11 Reuse of the Catalyst

Anti-microbial activity

Antimicrobial activity of the prepared BiVO₄ was determined by agar diffusion method on nutrient agar medium. The microbial strains like E.coli maintained on sterile nutrient agar at 3- 4° C. A loop of inoculum was transferred into 5ml of nutrient broth and incubated at 2hrs at 37°C. 1ml of these sample was spread on nutrient agar plate. Then, 4 wells were made in sterile nutrient agar plate cork borer. Then 50µl of solvent containing nanocomposite was placed in the wells made in nutrient agar plate. The treatment also includes as penicillin as positive control. The plate was incubated for 24hrs at 37°C and the zone of inhibition around the well was measured by 7.5-6.8mm. The effect of the material on bacteria have been studied by many research papers. In the present work, two different samples were used for antibacterial activity. The activity of BiVO₄ was higher against E.Coli bacteria[44-45].

CONCLUSION

The visible light driven BiVO₄ nanocrystals was synthesized by sonochemical method and the photocatalyst were characterized by various analytical methods like SEM-EDAX, XRD, FT-IR and UV-DRS spectra. The zero point charge of the photocatalyst will play a vital role in dye degradation. This result indicates that BiVO₄ nanocrystals, which are inducing the photodegradation of MB and Rh B dyes under sunlight irradiation. The synthesized BiVO₄ nanocrystals could be used for removal of wastewater which contributes to the environmental pollution.

ACKNOWLEDGEMENT

The authors would like to thank the UGC for providing funding to carry out this work and the Management of Ayya Nadar Janaki Ammal College, Sivakasi for providing lab facilities to carry out this research work. The author also thank the management of Dhanalakshmi Srinivasan College of Arts and Science for Women (A) for providing financial support.

REFERENCES

1. Dong, S., Feng, J., Fan, M., Pi, Y., Hu, L., Han, X., Liu, M., Sun, J., (2015). Recent developments in heterogegeous photocatalytic water treatment using visible-light responsive Photocatalysts : A review, *RSC Advances*, (5), 14610-14630.
2. Dong, S., Cui, Y., Wang, Y., Li, Y., Hu, L., Sun, J., (2014). Designing three-dimensional acicular sheaf shaped BiVO₄/reduced grapheme oxide composites for efficient sunlight-driven photocatalytic degradation of dye waste water, *Chem.Eng. Journal*, (249), 102-110.
3. Zhou, B., Qu, J., Zhao, X., Li, H., (2011). Fabrication and photoelectrocatalytic properties of nanocrystalline monoclinic BiVO₄ thin-film electrode, *J. Environ. Sci.*, (23), 151-159.
4. Gawnade, S.B., Thakare, S.R., (2012). Graphene wrapped BiVO₄ photocatalyst and its enhanced performance under visible light irradiation, *International Nanoletters*. (2), 11.
5. Payne, D.J., Robinson, M.D., Egdell, R.G., Walsh, A., Mc Nulty, J., Smith, K.E., Piper, L.F.J., (2011). The nature of electron lone pairs in BiVO₄, *Applied Physics Letters*. (98), 212110
6. Wang, X., Li, G., Ding, J., Peng, H., Chen, K., (2012). Facile synthesis and photocatalytic activity of monoclinic BiVO₄ micro/ nanostructures with controllable morphologies, *Mater. Res. Bull.* (47), 3814-3818.
7. Dong, S., Feng, J., Li, Y., Hu, L., Liu, M., Wang, Y., Pi, Sun, J., (2014). Shape-controlled synthesis of BiVO₄ hierarchical structures with unique-natural-sunlight-driven photocatalytic activity, *Appl. Cata. B : Environ.*, (152), 413-424.
8. Zhang, H.M., Liu, J.B., Wang, H., Zhang, W.X., Yan, H., (2008). Rapid microwave- assisted synthesis of phase controlled BiVO₄ nanocrystals and research on photocatalytic properties under visible light irradiation, *J. Nanopart Res*, (10), 767-774.
9. Bajaj, R., Sharma, M., Bahadur, D., (2013). Visible light-driven novel nanocomposite (BiVO₄/CuCr₂O₄) for efficient degradation of organic dye†, *Dalton Trans.* (42), 6736-6744.
10. Li, Z., Shen, Y., Yang, C., Lei, Y., Guan, Y., Lin, Y., Liu, D., Nan, C.W., (2013). Significant enhancement in the visible light photocatalytic properties of BiFeO₃-Graphene nanohybrids †, *J. Mater. Chem. A* (1), 823.
11. Xu, Y. S., De Zhang, W., (2013). Monodispersed Ag₃PO₄ nanocrystals loaded on the surface of spherical Bi₂MoO₆ with enhanced photocatalytic performance†, *Dalton Trans.* (42), 1094.
12. Zhang, X., Ai, Z., Jia, F., Fan, L., Zou, Z., (2007). Selective synthesis and visible-light photocatalytic activities of BiVO₄ with different crystalline phases, *Mater. Chem. Phys.* (103), 162-167.
13. Abdullah, A.H., Ali, N.M., Tahir, M.I.M., (2009). synthesis of bismuth vanadate as visible-light photocatalyst, *The Malaysian Journal of Analytical Sciences*. (13), 2 -10.
14. Dunkle, S.S., Helmich, R.J., Suslick, K.S., (2009). BiVO₄ as a Visible-Light Photocatalyst Prepared by Ultrasonic Spray Pyrolysis, *J. Phychem. C. Lett.* (113), 11980-11983.
15. Tojo, T., Zhary, Q.W., Saito, F., (2007). Spatial separation of photogenerated electrons and holes among {010} and {110} crystal facets of BiVO₄, *Chem. sustain. develop.* (15): 243-247.
16. Ma, Z.Y., Yao, B.H., (2013). Rapid microwave-assisted synthesis of phase controlled BiVO₄ nanocrystals and research on photocatalytic properties under visible light irradiation, *Chinese Journal of Chemical Physics*, (26), 3 -12.
17. Chen, L., Lladó, E., Hettick, M., Sharp, I.D., Lin, Y., Javey, A., Ager, J.W., (2013) Reactive Sputtering of Bismuth Vanadate Photoanodes for Solar Water Splitting, *J. Phys. Chem. C*, (1), 1-15.
18. Zhang, A., Zhang, J., (2009) The effect of hydrothermal temperature on the synthesis of monoclinic bismuth vanadate powders, *Mater. Sci- Poland*, (27), 1015-1023.
19. Ma, Z., Yao, B., (2013) Preparation of BiVO₄ Hollowspheres and its photocatalytic degradation of methylene Blue, *Chin. J. Chem. Phys.*, (26), 3-11.
20. Garcia-Perez, U.M., Sepulveda- Guzman, S., Cruz, AM., Peral, J., (2012) Selective Synthesis of Monoclinic Bismuth Vanadate Powders by Surfactant-Assisted Co-Precipitation Method: Study of Their Electrochemical and Photocatalytic Properties, *Int. J. Electrochem. Sci.*, (7), 9622-9632 .
21. Wu, S., Zheng, H., Lian, Y., Wu, Y., (2013). Preparation, characterization and enhanced visible-light photocatalytic activities of BiPO₄/BiVO₄ composites, *Mater. Res. Bull.* (48): 2901-2907.
22. Deshuang, W.L., Zhou, X., Zhang, Y., Yu, J., (2011). Preparation of BiVO₄@Fiber Composites and the Photocatalytic Property for Degradation of Organic Dyes under Visible-Light, *Green. Sustain. Chem.* (1), 98-102.
23. Zhou, Y., Jiang, G., Wang, R., Wang, R., Hu, R., Xi, X., (2012) Photocatalytic Activity of Hierarchically Nanoporous BiVO₄/TiO₂ Hollow Microspheres, *J. Fiber Bioengin. Inform.* (5), 181-190.
24. Ge, L., (2008). Novel Pd/ BiVO₄ composite Photocatalysts for efficient degradation of methyl orange under visible light irradiation, *Mater. Chem. Phy.* (107), 465-470.
25. Tamani, B., Heiran, R., Motazer, E.R., (2012). Modified polyacrylamide-supported chlorochromate as a new polymeric oxidizing agent, *J. Serb. Chem. Soc.* (77), 685-697.

26. Perkgoz, N.K., Toru, R.S., Uncl, E., Sefune, M.A., Tek, S., Muthugun, E., Soganci, I.M., Celiker, H., Celiker, Z., Demir, H.V., (2011). photocatalytic hybrid nanocomposite of metaloxide nanoparticles enhanced towards the visible spectral range, *Appl. Catal. B Environ.* (105), 77-85.
27. Muthirulan, P., Meenakshi Sundaram, M., Kannan, N., (2012). Beneficial role of ZnO photocatalyst supported with porous activated carbon for the mineralization of alizarin cyanin green dye in aqueous solution, *J. Adv Res*, (1), 1-6.
28. Muthirulan, P., Nirmala Devi, C., Meenakshi Sundaram, M., (2012). Synchronous role of coupled adsorption and photocatalytic degradation on CAC-TiO₂ composite generating excellent mineralization of alizarin cyanine green dye in aqueous solution, *Arab. J. Chem.*, (1), 1-7.
29. Solomon, R.V., Lydia, S., Merlin, J.P., Venuvalingam, P., (2012). Enhanced photocatalytic degradation of azo dyes using Fe₃O₄, *J. Iran. Chem. Soc.* (1), 1-10.
30. Natarajan, T.S., Natarajan, K., Bajaj, H.C., Tayade, R.J., (2013). Enhanced photocatalytic activity of bismuth-doped TiO₂ nanotubes under direct sunlight irradiation for degradation of Rhodamine B dye, *J. Nanopart Res.* (15), 1669.
31. Sharma, D., Bansal, A., Ameta, R., (2011). Sharma, H.S., Comparison of efficiency of APM and MnO₂ by photocatalytic degradation of Azure-B based on quality parameter modification, *IJCRGG* (3), 1008-1014.
32. Sharma, S., Ameta, R., Malkani, R.K., Ameta, S.C., (2013). photocatalytic degradation of rose Bengal using semiconducting zinc sulphide as the photocatalyst, *J. Serb. Chem. Soc.* 78 (6), 897-905.
33. Wang, P., Tang, Y., Dong, Z., Chen, Z., Lim, T.T., (2013). Ag-AgBr/ TiO₂/RGO nanocomposites for visible-light photocatalytic degradation of Penicillin G, *J. Mater. Chem. A*, (1), 4718.
34. Appel, C., Lena, Q., Dean Rhue, R., Kennelley, E., (2013). Point of zero charge determination in solids and minerals via traditional methods and detection of electroacoustic mobility, *Geoderma*, (113), 77-93.
35. Appel, L.Q., (2002). Concentration, pH and surface charge effects on cadmium and lead sorption in three tropical soils, *J. Environ. Qual.* (31), 581-589.
36. Atkinson, R.J., Posner, A.M., Quirk, J.P., (1967). The film-forming abilities of iron oxides and oxyhydroxides, *J. Phys. Chem.* (71), 550-558.
37. Braggs, B., Fornasiero, D., Ralston, J., Smart, R.S., (1994) Characterization of surface-modified montmorillonite nanocomposites, *Clay Miner.* (42): 123-136.
38. Chorover, J., Sposito, G., (1995). Colloquium on geology, mineralogy and human welfare, *Geochim. Cosmochim. Acta*, (59), 875-884.
39. Huang, H., He, Y., Lin, Z., Kang, L., Zhang, Y., (2013). Two novel bi-based borate photocatalysts: Crystals structure, electronic structure, photoelectrochemical properties and simulated solar light irradiation, *J. Phys. Chem. C* (117), 22986-22994.
40. Obregon, S., Lee, S.W., Colon, G., (2014). Exalted photocatalytic activity of tetragonal BiVO₄ by Er³⁺ doping through a luminescence cooperative mechanism, *Dalton Trans.* (43), 311.
41. Wang, J., Osterloh, F.E., (2014). Limiting factors for photochemical charge separation in BiVO₄/Co₃O₄, a highly active photocatalyst for water oxidation in sunlight, *J. Mater. Chem. A*, (2), 9405.
42. Park, H.S., Ha, H.W., Ruoff, R.S., Bard, A.J., (2014). The improvement of photo electro chemical performance and finite element analysis of reduced graphene oxide-BiVO₄ composite electrodes, *Journal of Electroanalytical Chemistry*, (716), 8-15.
43. Wetchakin, N., Chaiwichain, S., Inceesungvoln, B., Pingmuang, K., Phanichphant, S., Minett, A.I., (2012). BiVO₄/CeO₂ nanocomposites with high visible-light induced photocatalytic activity, *J. Chem. Appl. Mater. Interface*, (4), 3718-3723.
44. Obregon, S., Colon, G., (2013). On the different photocatalytic performance of BiVO₄ catalysts for Methylene Blue and Rhodamine B degradation, *J. Mol. Catal. A: Chem.* (376), 40-47.
45. Castelli, N.S., Heel, A.H., Graule, T., Pulgarin, C., (2010). Flame-assisted synthesis of nanoscale, amorphous and crystalline, spherical BiVO₄ with visible light photocatalytic activity, *Appl. Catal. B: Environ.* (95), 335-347.

CITATION OF THIS ARTICLE

M. Sangareswari, S. Arul Manikandan, T. Adinaveen, S. Srinivasan, S. Sathyakumar, M. Srinivasan, P. Ganapathy and Jiji George: Antimicrobial and Photo Degradation Activity Of Synthesized BiVO₄ Nanocrystals. *Bull. Env. Pharmacol. Life Sci.*, Spl Issue [5]: 2022: 551-559.